Journal of Applied Fluid Mechanics, Vol. 12, No. 4, pp. 1265-1272, 2019.
Available online at www.jafmonline.net, ISSN 1735-3572, EISSN 1735-3645.
DOI: 10.29252/jafm.12.04.29614

Capillary Wave and Initial Spreading Velocity at Impact of Drop onto a Surface

P. F. Li, S. F. Wang and W. L. Dong

College of Energy and Power Engineering, Nanjing University of Aeronautics and Astronautics, Nanjing 210016, China

†*Corresponding Author Email: sfwang@nuaa.edu.cn*

(Received September 6, 2018; accepted December 4, 2018)

ABSTRACT

The capillary wave and initial spreading velocity in the spreading phase of drop impacting on a glass surface are studied experimentally, while the drop photos are obtained by using a high-speed video camera, which can catch up to 9000 images per second with an exposure time of 4 μs. A wide range of impact velocities are studied by varying the fall height, showing different capillary waves. All attention is given to the capillary wave and initial spreading velocity of drop. A non-linear relation between the wavelength and the impact velocity is found experimentally. Combined with the minimum spreading radius theory, a linear relation between the initial spreading velocity and the impact velocity is acquired.

Keywords: Drop impact; Capillary wave; initial spreading velocity; Impact velocity; Contact line.

NOMENCLATURE

a_n	*n=1, 2, 3. Constant*
c	wave velocity
C_f	*friction coefficient*
D_0	*equivalent drop diameter*
D(t)	spreading diameter
E_k	kinetic energy of capillary wave
R(t)	spreading radius
f	*wave frequency*
g	*gravitational constant*
H	*fall height of the drop*
H_1	*liquid depth*
L_0	*horizontal radius of the bubble*
V_i	impact velocity of the drop
V_0	initial spreading velocity
V(t)	spreading velocity
We	Weber number
γ	surface tension for the water-air interface
λ	*Wavelength of capillary wave*
μ_{water}	viscosity of water
μ_{air}	viscosity of air
ρ_{water}	density of water
ρ_{air}	air density

1. INTRODUCTION

The phenomenon of drop impacting on a dry surface has been seen in many industries, such as aerospace (Farrall *et al.* 2007), aviation (Jones *et al.* 2014), agricultural (Bergeron *et al.* 2000), spray painting (Mcdonald *et al.* 2006), printed electronics with spray coating (Eslamian, 2014; Soltani-Kordshuli and Eslamian, 2017) and inkjet printing (Dam, 2004). The impact may result in the drop rebounding over the solid surface, spreading, even splashing (Yarin, 2005; Rioboo *et al.* 2001).Many parameters have great influence on the outcome of drop impact, such as drop size, impact velocity (Visser *et al.* 2012; Feng, 2017), the viscosity and surface tension of the liquid (Bergeron *et al.* 2000), the roughness (Lee, 2016b) and wettability of the solid surface (Romdhani *et al.* 2014; Kai and Feuillebois 1998; Lee, 2014a), impact angle (Mitra *et al.* 2013), environment temperature (Gumulya, 2015) and pressure (Xu *et al.* 2005, Xu 2007)etc.

1.1 Capillary Waves

After drop impacting on surface, capillary waves propagate on the surface of the drop from the bottom to the top of the drop. Due to the short impact time, there will be a number of short waves moving along the surface of the drop. These waves are also called capillary waves.

Lesser (1981) first proposed that shockwaves will occur when drops impact the wall. Later, several scholars (Lesser and Field 1983; Field, 1985; Dear and Field, 1988; Rioboo, 2002) analyzed the duration of the shock generation by theoretical methods. Rouex (2004) explicitly indicated shockwave in the form of capillary waves propagate on the surface of the drop from the bottom to the top of the drop.

Renardy (2003) believed that the wave velocity of the capillary wave in the drop is equal to the drop impact velocity and the corresponding capillary wavelength is obtained. He only analyzes the surface waves of macroscopic drops. However, the shockwave should trigger a lamella ejection at the moment of impact (Lesser and Field, 1983; Field, 1985; Dear and Field, 1988). The moment of shockwave detachment calculated for impact velocities of a few meters per second is only a few nanoseconds. So the surface waves generated by shockwaves should be capillary waves with shorter wavelengths. Renardy (2003) provided a method for calculating the wavelength of surface waves. Due to the limitations of experimental conditions, Renardy (2003) could not obtain photos close to the capillary waves. In this article, the capillary waves with shorter wavelengths are observed by experiments.

1.2 Spreading Velocity

Lee (2016a) proposed an improved energy balance model for maximum spreading ratio based on a correct analytical modeling of the time at max dissipation, and other improvement was based on the use of the dynamic contact angle at maximum spreading, instead of quasi-static contact angles, to describe the dynamic wetting process at low impact velocity.

A study on the initial spreading velocity for a water drop impinging on glass and parafilm surfaces was performed using a fast-speed video camera system by Hung (2011), and one of the experimental results fit well with the empirical equation of Roux (2004). Bouwhuis (2012) revealed there must exist an impact velocity of the liquid drop in which the size of this entrained air bubble was maximal.

So when the drop impacts on the surface, the air between the drop and the wall makes the dent on the drop bottom side and forms a small bubble in Fig. 1. This causes the drop to be in contact with the wall as a closed contact line, but not a single point, and the contact line has initial spreading velocity. Since the effect of drop replenishment bubbles is not considered, Roux (2004) believed that initial spreading velocities were equal to 4.8 times impact velocities. In reality, initial spreading velocities should be less than 4.8 times impact velocities.

The spreading of a liquid drop can be decomposed into four phases: a kinetic phase, a spreading phase, a relaxation phase and a wetting phase (Rioboo, 2002; Roux, 2004). In this article, the dynamics of water drop impacting on a smooth glass surface is studied in detail. The manual measurement error is reduced by using spreading diameter measurement program and a new method to calculate the initial spreading velocity of water drop impact is provided based on the maximum bubble capture theory.

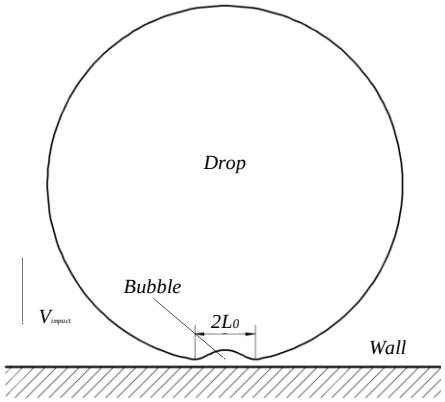

Fig. 1. Characterization of air bubble entrapment.

2. EXPERIMENTAL PART

The experimental set-up is constructed to allow the impact of single drop onto a smooth glass surface, to be studied with high temporal and spatial resolution. Figure 2 shows the experimental set-up. The main components of the experimental apparatus are the high-speed camera (*IDT Y5, 2336×1728 pixels*), lamp, lifting platform, computer and syringe pump.

The high-speed digital camera is used to capture the images of drop impact on the particle. Since the image resolution varies inversely to the capturing frame rate, therefore, the frame rate and shutter speed are optimized to obtain the best possible image. The typical frame rate and exposure time used in the experiments are 9000 *fps* and 4 μs. The camera was placed parallel to the impact surface at a zero degree angle to the setup. This arrangement allowed the best view of the liquid–solid interaction at the interface.

A 20 *ml* syringe is placed in a syringe pump and used as the drop delivery system. The stroke length of the syringe pump is adjusted to allow a single drop to fall onto the impacting surface. The same batch of slides is used as the impact plane in the experiment for reducing the influence of surface roughness and rapid experiment. Also, in order to avoid contamination of the glass due to the possible residue left by previous drops, we replaced the substrate with a fresh slide after every measurement.

The impact velocity is adjusted by changing the height of the drop and the glass surface. In order to obtain a uniform light source, a soft light paper should be placed in front of the lamp. The spread drop diameter from the captured images was measured by means of a self-developed *MATLAB* code.

In the present study experimental data on the apparent a distilled water drop (D = 3.8 *mm*)

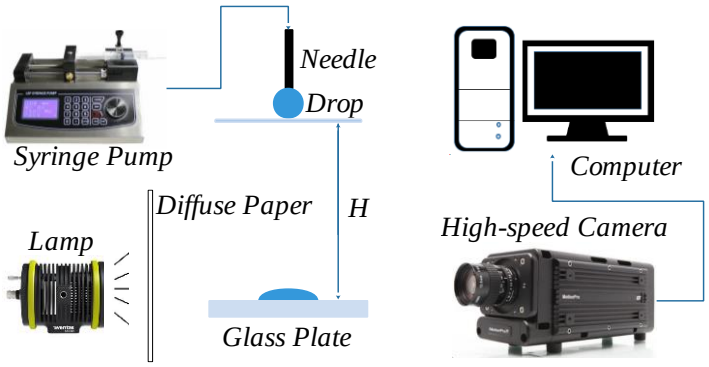

Fig. 2. Schematic representation of drop impact experimental setup.

spreading on a horizontal surface are presented. Based on the resolution (960×163 *pixels*) of the images, both measurements of the impacting drop diameter were estimated to be accurate within ±3%. The drop's initial diameter is the same for all the experiments whereas the impact velocity ranges from 0.61 to 4.28 *m/s* (*We*=19~958).

The instantaneous impact velocity of a drop can be estimated by the empirical equation (Kai, 1998) and the empirical friction coefficient C_f of this paper is 0.866.

$$V_i = \sqrt{\frac{4g\rho_{water}D_0}{3C_f\rho_{air}}\left(1-\exp(-\frac{3C_f\rho_{air}H}{2\rho_{water}D_0})\right)} \quad (1)$$

3. Results And Discussion

3.1 Characteristics of Capillary Waves

For showing the spreading time dependence at spreading images in Fig. 3, we report the spreading images versus time for two impact velocities. The dependence of drop shape on time with the impact velocities equal to 0.611*m/s* and 1.14 *m/s* are shown in the images respectively. At the first stage of impact, the drop and the plate are in contact at a circle line defining the contact line. When spreading occurs, the radius of the contact line will gradually increase with the spreading time until the maximum spreading radius is met. Meanwhile, the shapes of water drops often change from spheroid to cap shape, and then to be disk shape.

As the impact velocities increases, the spread time of the maximum spreading radius decreases gradually. The drops are respectively stretched, compressed and spherical before they impact on surface, since the drops have a certain oscillation frequency after breaking away from the needle.

In Fig. 3, it can be observed that there is a capillary wave near the wall at a certain moment. In Figs. 4 (a), (b) and (c) are drop spread images at a certain time of three impact velocities, respectively. For facilitating the observation of the capillary waves in the drops, the capillary waves at a certain moment are separately shown in Fig. 4. According to the analysis in Section 1.1, we consider the capillary wave to be the capillary wave generated by the drop impact shockwave. In the experiment, the drop diameters of 2.6 *mm* and 2.0 *mm* are also tested, but no capillary waves are observed in the drops, which may be easier to observe due to the large diameter drops.

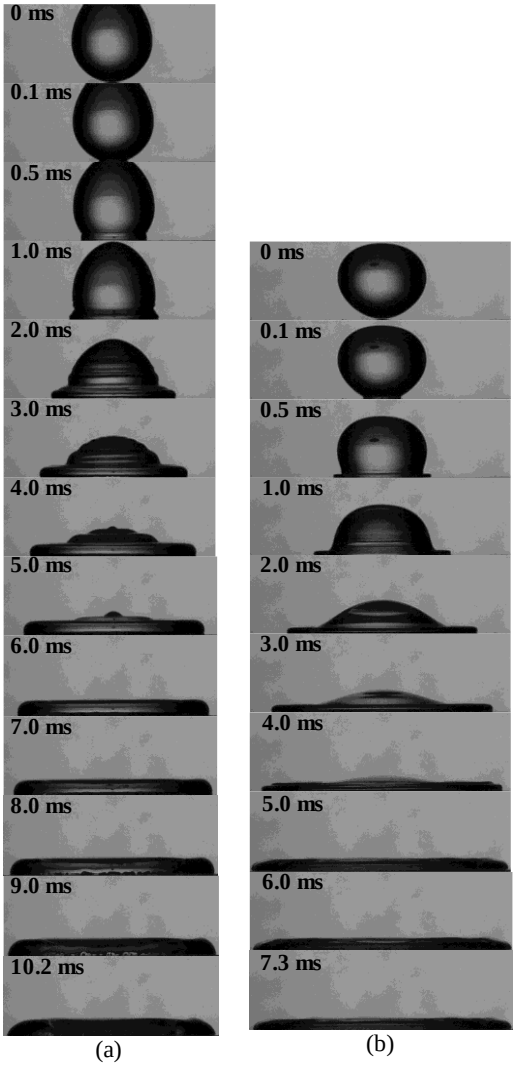

(a) (b)

Fig. 3. Series of drop spreading images for impact velocity: (a), V_i = 0.611*m/s* and (b), V_i = 1.14*m/s*.

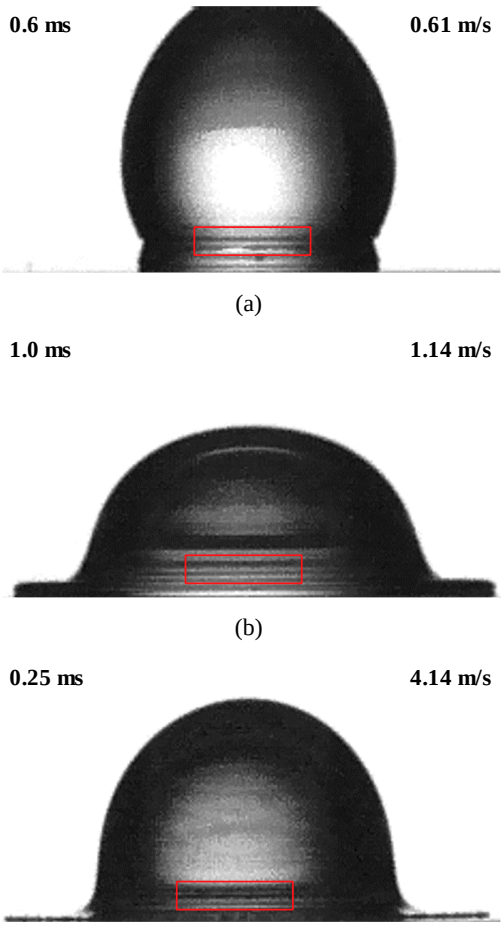

Fig. 4. The capillary waves of the drops at a certain moment.

In Fig. 3(a), when the drop impacts on the wall at a low velocity, it appears to have obvious stratification, which may be caused by the spreading speed of the drop being too slow, resulting in the spreading speed of the upper layer of the drop being greater than the spreading speed of the lower layer, and then the phenomenon of layered spreading occurs. In Fig. 4, it can be observed by enlarging the spreading image that the higher the impact velocity of the drops, the smaller the ripples, and the time at which the capillary waves appear first increases and then becomes shorter.

3.1.1 Wavelength

During the experiment, the exposure time is small enough to ensure that the waveforms do not overlap. The angle between the impact surface and the camera is 0 degrees, which can show a clear waveform. An image of the first occurrence of capillary waves in a set of spread images is selected to measure the wavelength.

Durst (2008) believes that the kinetic energy of capillary waves is proportional to the square of the wave velocity.

$$E_k \propto c^2 \tag{2}$$

Literatures (Yih, 1969; Currie, 2002; Durst, 2008) all consider the wave velocity and wavelength of capillary waves present a certain relationship.

$$c^2 = 2\pi\gamma/(\rho_{water}\lambda) \tag{3}$$

Therefore, kinetic energy is negatively correlated with wavelength.

$$E_k \propto 1/\lambda \tag{4}$$

As shown in Eqs. (2) – (4), the energy is gradually dissipated during capillary waves progress from the bottom to the top of the drop, so that the wavelength of the capillary waves becomes longer. And to avoid the interference of the foot thickness on the wavelength measurement, the wavelength close to the wall but above the foot thickness should be selected.

In Fig. 5, with the impact velocity increases, the wavelength gradually decreases and tends to a certain value. The wavelength is much smaller than the drop diameter. When the impact velocity is higher than 1.14 *m/s*, the drop spreads into a cap shape, and capillary waves can be observed. The experimental results show that the maximum wavelength is 0.127 *mm* at 0.61 *m/s* and the minimum wavelength is 0.080 *mm* at 4.14 *m/s*.

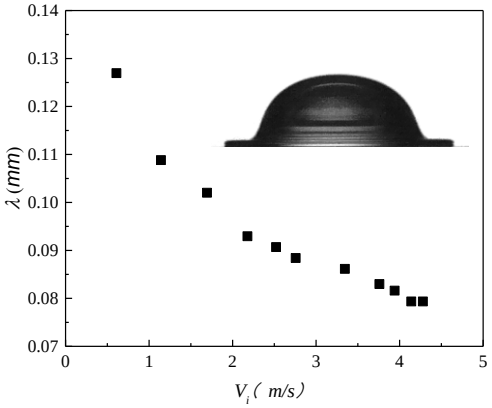

Fig. 5. Wavelengths versus the different impact velocities.

There is a limit at a certain speed due to the resistance of the drop. Therefore there is a minimum wavelength and it should be less than 0.082 *mm*. The reason will be given in section 3.1.3. When the impact velocity is 0.61- 4.28 *m/s*, the wavelength of the capillary wave is less than 0.13 *mm*. The wavelengths are much smaller than the wavelength of the gravity wave. The size of each pixel in the picture taken by the high-speed camera is 0.027*mm**0.027*mm*. To reduce the measurement error of the wavelength, the picture is magnified 3 times by MATLAB software and the size of each pixel is 0.009*mm**0.009*mm*. Therefore, the measurement error of the wavelength is in the range of 7.2% to 11.1%.

3.1.2 Wave Velocity and Wave Frequency

In Eq. (3), the wave velocity is significantly

affected by the surface tension. When H_1/λ is greater than 10, it is a deep water wave. Since the diameter of the droplet is 3.799 *mm* and the range of D_0/λ is 29.9 ~ 47.9, the wave velocity can be calculated by Eq. (3). For waves with small wavelengths, the capillary effects dominate (Currie, 2002), and the influence of gravity can be ignored at this time.

The capillary wave is generated instantaneously by the drop impacting on the wall. It is measured from Fig. 4 that the wavelengths of two adjacent waves are the same, so the capillary wave should be a monochromatic wave. Therefore, the wave frequency can be expressed by the wave velocity and the wavelength.

$$f = c/\lambda \tag{5}$$

The wave velocity of the capillary wave at the corresponding wavelength can be obtained by Eq. (3). Figure 6 shows the relationship between wave velocity and wave frequency with impact velocity. Both the wave velocity and the wave frequency increase as the impact velocity increases. When the impact velocity is 0.61 *m/s*, the minimum wave velocity is 1.90 m/s, and when the impact velocity is 4.14 *m/s*, the maximum wave velocity is 2.40 *m/s*.

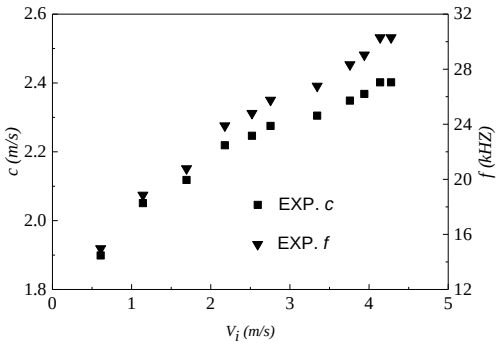

Fig. 6. Wave Velocities and Wave Frequencies versus the different impact velocities.

When the impact velocity is between 0.16 and 4.28 *m/s*, the wave frequency of the capillary wave is greater than 14.957 *kHZ*. From this, it can be inferred that the action between the drop and the wall surface in the initial stage of the drop impacting on the wall surface is so intense that the capillary waves are high-frequency waves.

3.1.3 Critical Impact Velocity

Figure 7 shows the relationship between the ratio of wave velocity and the corresponding impact velocity as a function of the impact velocity, which can be described by Power function or allometric function.

$$\frac{c}{V_i} = 2.01\, V_i^{-0.88} \tag{6}$$

Renardy (2003) proposed a range of velocities for which the capillary waves occur in Eq. (7). According to Eq. (7), when the drop diameter is 3.8 *mm*, the impact velocity should be less than 1.4 *m/s*, but when the impact velocity is greater than 1.4 *m/s*, we also observed capillary waves.

$$\left(\frac{2\gamma}{\rho_{water} D_0}\right)^{1/2} < V_i < \left(\frac{2\gamma^2}{\mu_{water}\rho_{water} D_0}\right)^{1/3} \tag{7}$$

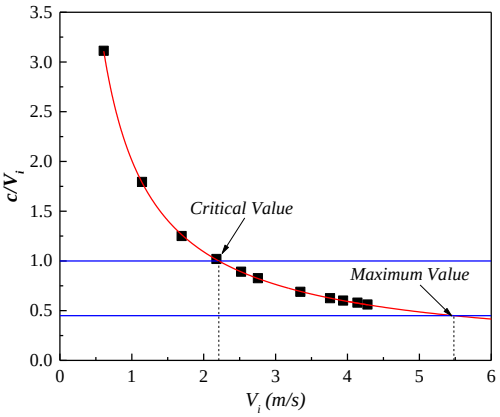

Fig.7. Ratio of wave velocity to the corresponding impact velocity versus the different impact velocities.

The range of impact velocity which the capillary wave may be observed is given in Fig. 7. At low-speed impacts, the wave velocity of the capillary wave is much larger than the impact velocity, and easily to observe the capillary wave at spreading images. It can be found by Eq. (6) that when c/V_i = 1, V_i = 2.21*m/s*. When the impact velocity reaches a critical value (V_i = 2.21*m/s*), the wave velocity of the capillary wave is equal to the impact velocity, and the capillary wave can be observed at the initial moment of the drop impact. The greater the impact velocity, the less likely the capillary wave is observed. When the impact velocity reaches a certain extreme value, the impact velocity is much higher than the wave propagation velocity. Although the impact produces capillary waves, the images with capillary waves cannot be captured with a high-speed camera. The extreme value is defined as the maximum impact velocity at which the capillary wave appears.

3.2 Initial Spreading Velocity

Figure 8 reports the relation of spreading radius versus expanding time during the spreading diameters reach the maximum. As the drop spread asymmetrically, the spreading radius is used to describe the process of drop spreading. The spreading radius will typically grow quite quickly, then grow slowly and finally reach maximum values. It tends to take longer for low-speed drops to reach maximum expanding.

According to Section 1.2, there is an initial spreading speed when the spreading radius of the drop is equal to the radius of the bubble. Hicks (2012) gave empirical formulas for bubble radius and impact velocity through experimental and theoretical methods, as shown in Eq. (8), which was then experimentally verified by Liu (2012).

Table 1 Minimum spreading radius, Minimum spreading radius and Initial Spreading Velocity in different impact velocities

V_i (m/s)	L_0 (mm)	a_1	a_2	a_3	V_0(m/s)	V_0/V_i
0.61	0.286	1.16	1.52	0.710	2.71	4.43
1.14	0.232	2.12	2.21	0.543	5.20	4.55
2.18	0.187	3.53	2.95	0.418	9.17	4.21
2.52	0.178	4.37	2.86	0.351	12.38	4.91
2.76	0.173	4.33	3.45	0.405	11.52	4.18
3.76	0.156	5.51	3.49	0.369	16.17	4.30
4.14	0.151	5.73	3.83	0.279	16.41	3.96
4.28	0.150	6.08	3.80	0.304	18.11	4.23

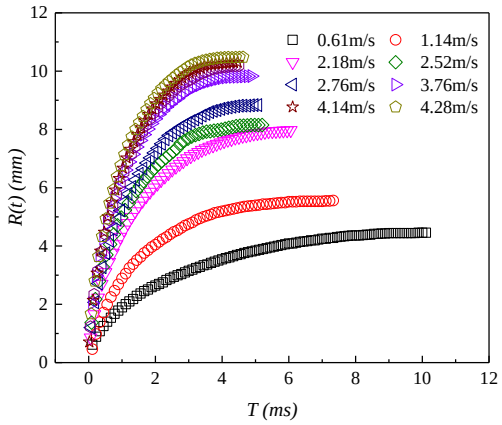

Fig. 8. Evolution with time of average spreading radius.

$$L_0 = 3.8\left(\frac{4\mu_{air}}{\rho_{water}V_i}\right)^{1/3}\left(\frac{D_0}{2}\right)^{2/3} \tag{8}$$

The bubble radius is related to the viscosity of the gas, the density of the drop, the impact velocity, and the initial diameter. The bubble radius decreases gradually with the rise of the impact velocity.

To accurately describe the initial stage of drop spreading, the curve fitting can be performed on the first 20 data points of each working condition in Fig. 8.

$$R(t) = a_1 + a_2 \ln(t + a_3) \tag{9}$$

Differential coefficient for the spreading radius versus time is equal to the spreading speed.

$$V(t) = R'(t) = \frac{a_2}{t + a_3} \tag{10}$$

The bubble radius calculated by Eq. (8) is taken into Eq. (9) to find the initial spreading time t_0, and then the initial spreading speed is obtained by Eq. (10).

The initial spreading velocity can be obtained according to Eqs. (8 - 10), then the ratio of the initial spreading velocity to the corresponding impact velocity is obtained. Table 1 shows the initial spreading velocity of drop in different impact velocities.

To reduce the deviation and acquire an accurate speed ratio, the arithmetic mean of the speed ratios whose relative deviation absolute values are less than 5% is taken. Therefore, excluding the condition of the impact velocities of 2.52 *m/s* and 4.14 *m/s*, the remaining speed ratios are calculated as the arithmetic mean value. There should be a specific functional relationship between the initial spreading velocity and the corresponding impact velocity, which is shown Eq. (11).

$$V_0 = 4.3V_i \tag{11}$$

Since the effect of drop replenishment bubbles has not been considered by Roux (2004) and Hung (2011), this paper combines the initial spreading velocity with the minimum spreading radius theory for the first time. The initial spreading velocity of water drop on the glass surface should be 4.3 times the impact velocity, which is less than 4.8 times from Roux (2004) and Hung (2011).

4. CONCLUSIONS

The capillary wave of a drop of water impacting a glass surface for various velocities of impact was experimentally studied. A detailed description of capillary wave during the spreading event is given.

Three important characteristic parameters of capillary waves are studied, which are wavelength, wave velocity and wave frequency. The wavelength is directly obtained by numerical image processing of the experimental photograph, and it is found that the wavelengths of the capillary waves generated by the impact are less than or equal to the submillimeter wave.

The wave velocity and the wave frequency of the capillary wave increase with the impact velocity. There is a critical point that the wave velocity is equal to the impact velocity, and then as the impact velocity increases, the capillary wave disappears in the spread image when the impact velocity reaches a maximum value.

The fluctuation energy equation and potential energy equation of surface wave were given by Yih (1969) and Durst (2008). However, the fluctuation energy equations of both have a slight difference. Since the amplitude of the capillary wave cannot be measured, the energy of the capillary wave cannot be calculated.

The spreading process of drop at room temperature on smooth glass surface is experimentally

investigated. The program based on *Matlab* software can be used to quickly handle and analyze the spreading radii of drop. The initial spreading velocity of water drop on the glass surface should be 4.3 times the impact velocity, which is less than 4.8 times.

ACKNOWLEDGMENT

Thanks to Associate Professor Liu for his contribution to the experimental image processing method.

REFERENCES

Bergeron, V. V., D. Bonn, J. Y. Martin and L. Vovelle (2000). Controlling drop deposition with polymer additives. *Nature* 405, 772.

Bouwhuis, W., R. C. A. V. D. Veen, T. Tran, D. L. Keij, K. G. Winkels, I. R. Peters, D. van der Meer, C. Sun, J. H. Snoeijer and D. Lohse (2012). Maximal air bubble entrainment at liquid-drop impact. *Physical Review Letters* 109, 264501.

Currie, I. G. and I. G. Currie (2002). *Fundamental Mechanics of Fluids, Third Edition*, Russia.

Dam, D. B. V. and C. L. Clerc (2004). Experimental study of the impact of an ink-jet printed drop on a solid substrate. *Physics Fluids* 16, 3403-3414.

Dear, J. P. and J. E. Field (1988). High-speed photography of surface geometry effects in liquid/solid impact. *Journal of Applied Physics* 63, 1015–1021.

Durst, F. and I. Arnold (2008). Fluid mechanics: an introduction to the theory of fluid flows. *Springer Berlin* 46, 123–131.

Eslamian, M. (2014). Spray-on Thin Film PV Solar Cells: Advances, Potentials and Challenges. *Coatings* 4, 60-84.

Farrall, M., S. Hibberd and K. Simmons (2007). The effect of initial injection conditions on the oil drop motion in a simplified bearing chamber. *Journal of Engineering for Gas Turbines and Power* 130, 012501.

Feng, J. Q. (2017). A computational study of high-speed microdrop impact onto a smooth solid surface. *Journal of Applied Fluid Mechanics* 10, 243-256.

Field, J. E., M. B. Lesser and J. P. Dear (1985). Studies of two-dimensional liquid wedge impact and their relevance to liquid-drop impact problems. *Proceedings of the Royal Society of London. Series A* 401, 225–249.

Gumulya. M., R. P. Utikar, V. Pareek, R. Mead-Hunter, S. Mitra and G. M. Evans (2015). Evaporation of a droplet on a heated spherical particle. *Chemical Engineering Journal* 278, 309-319.

Hicks, P. D., E. V. Ermanyuk, N. V. Gavrilov and R. Purvis (2012). Air trapping at impact of a rigid sphere onto a liquid. *Journal of Fluid Mechanics* 695, 310-320.

Hung, Y. L., M. J. Wang, Y. C. Liao and S. Y. Lin (2011). Initial wetting velocity of drop impact and spreading: Water on glass and parafilm. *Colloids and Surfaces A* 384, 172-179.

Jones, W. P., A. J. Marquis and K. Vogiatzaki (2014). Large-eddy simulation of spray combustion in a gas turbine combustor. *Combus. Flame* 161, 222-239.

Kai, R. and F. Feuillebois (1998). Influence of surface roughness on liquid drop impact. *Journal of Colloid and Interface Science* 203, 16-30.

Lee, J. B., D. Derome, R. Guyer and J. Carmeliet (2016a). Modeling the maximum spreading of liquid drops impacting wetting and nonwetting surfaces. *Langmuir* 32, 1299.

Lee, J. B., N. Laan, K. G. de Bruin, G. Skantzaris, N. Shahidzadeh, D. Derome, J. Carmeliet and D. Bonn (2016b). Universal rescaling of drop impact on smooth and rough surfaces. *Journal of Fluid Mechanics* 786, R4

Lesser, M. B. (1981). Analytic Solutions of Liquid-Drop Impact Problems. *Proceedings of the Royal Society of London* 377, 289-308.

Lesser, M. B. and J. E. Field (1983). The impact of compressible liquids. *Annual Review of Fluid Mechanics* 15, 97–122.

Liu, Y., P. Tan and L. Xu (2012). Compressible air entrapment in high-speed drop impacts on solid surfaces. *Journal of Fluid Mechanics* 716, 643-669.

Mcdonald, A., M. Lamontagne, C. Moreau and S. Chandra (2006). Impact of plasma-sprayed metal particles on hot and cold glass surfaces. *Thin Solid Films* 514, 212-222.

Mitra, S., M. J. Sathe, E. Doroodchi, R. Utikar, Milin K. Shah, V. Pareek, J. B. Joshi and G. M. Evans (2013). Droplet impact dynamics on a spherical particle. *Chemical Engineering Science* 100, 105-119.

Renardy, Y., S. Popinet, L. Duchemin, M. Renardy, S. Zaleski, C. Josserand, M. A. Drumright-Clarke, D. Richard, C. Clanet and D. Quéré(2003). Pyramidal and toroidal water drops after impact on a solid surface. *Journal of Fluid Mechanics*484, 69-83.

Rioboo, R., M. Marengo and C. Tropea (2001). Outcomes from a drop impact on solid surfaces. *Atomization and Sprays* 11, 155-166.

Rioboo, R., M. Marengo and C. Tropea (2002). Time evolution of liquid drop impact onto solid, dry surfaces. *Experiments in Fluids* 33, 112-124.

Romdhani, Z., A. Baffoun, M. Hamdaoui and S. Roudesli (2014). Drop impact on textile material: effect of fabric properties. *Autex Research Journal*14, 145-151.

Roux, D. C. and J. J. Cooper-White (2004). Dynamics of water spreading on a glass surface. *Journal of Colloid and Interface Science* 277, 424-436.

Soltani-Kordshuli, F. and M. Eslamian (2017). Impact dynamics and deposition of pristine and graphene-doped PEDOT: PSS polymeric droplets on stationary and vibrating substrates. *Experimental Thermal and Fluid Science* 89, 238-248.

Visser, C. W., Y. Tagawa, C. Sun and D. Lohse (2012). Microdrop impact at very high velocity. *Soft Matter* 8, 10732-10737.

Xu, L. (2007). Liquid drop splashing on smooth, rough, and textured surfaces. *Physical Review E* 75, 056316.

Xu, L., W. W. Zhang and S. R. Nagel (2005). Drop splashing on a dry smooth surface. *Physical Review Letters* 94, 184505.

Yarin, A. L. (2005). Drop impact dynamics: splashing, spreading, receding, bouncing. *Annual Review of Fluid Mechanics* 38, 159-192.

Yih, C. (1969). *Fluid mechanics: a concise introduction to the theory*. Mcgraw-HILL Book Company.